AUTHOR(S): WANG, S.-L., FERNANDEZ, C., ZOU, C.-Y., YU, C.-M., CHEN, L. and ZHANG, L.

TITLE: A comprehensive working state monitoring method for power battery packs considering state of balance and aging correction.

YEAR: 2019

Publisher citation: WANG, S.-L., FERNANDEZ, C., ZOU, C.-Y., YU, C.-M., CHEN, L. and ZHANG, L. 2019. A comprehensive working state monitoring method for power battery packs considering state of balance and aging correction. Energy [online], 171, pages 444-455. Available from: https://doi.org/10.1016/j.energy.2019.01.020

OpenAIR citation: WANG, S.-L., FERNANDEZ, C., ZOU, C.-Y., YU, C.-M., CHEN, L. and ZHANG, L. 2019. A comprehensive working state monitoring method for power battery packs considering state of balance and aging correction. Energy, 171, pages 444-455. Held on OpenAIR [online]. Available from: https://openair.rgu.ac.uk/

Accepted Manuscript

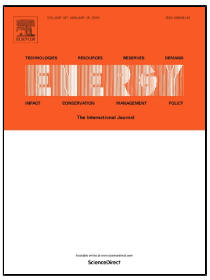

A comprehensive working state monitoring method for power battery packs considering state of balance and aging correction

Shun-Li Wang, Carlos Fernandez, Chuan-Yun Zou, Chun-Mei Yu, Lei Chen, Li Zhang

PII:	S0360-5442(19)30022-2
DOI:	10.1016/j.energy.2019.01.020
Reference:	EGY 14493
To appear in:	*Energy*
Received Date:	26 June 2018
Accepted Date:	05 January 2019

Please cite this article as: Shun-Li Wang, Carlos Fernandez, Chuan-Yun Zou, Chun-Mei Yu, Lei Chen, Li Zhang, A comprehensive working state monitoring method for power battery packs considering state of balance and aging correction, *Energy* (2019), doi: 10.1016/j.energy.2019.01.020

A comprehensive working state monitoring method for power battery packs considering state of balance and aging correction

Shun-Li Wang[a], Carlos Fernandez[b], Chuan-Yun Zou[a], Chun-Mei Yu[a*], Lei Chen[a], Li Zhang[a]

[a]*School of Information Engineering & Robot Technology Used for Special Environment Key Laboratory of Sichuan Province, Southwest University of Science and Technology, Mianyang 621010, China;*
[b]*School of Pharmacy and Life Sciences, Robert Gordon University, Aberdeen AB10-7GJ, UK.*

Abstract: A comprehensive working state monitoring method is proposed to protect the power lithium-ion battery packs, implying accurate estimation effect but using minimal time demand of self-learning treatment. A novel state of charge estimation model is conducted by using the improved unscented Kalman filtering method, in which the state of balance and aging process correction is considered, guaranteeing the powered battery supply reliability effectively. In order to realize the equilibrium state evaluation among the internal battery cells, the numerical description and evaluation is putting forward, in which the improved variation coefficient is introduced into the iterative calculation process. The intermittent measurement and real-time calibration calculation process is applied to characterize the capacity change of the battery pack towards the cycling maintenance number, according to which the aging process impact correction can be investigated. This approach is different to the traditional methods by considering the multi-input parameters with real-time correction, in which every calculation step is investigated to realize the working state estimation by using the synthesis algorithm. The state of charge estimation error is 1.83%, providing the technical support for the reliable power supply application of the lithium-ion battery packs.

Keywords: *power battery pack; working state monitoring; unscented Kalman filter; state of balance; aging correction*

Corresponding author: Chun-Mei Yu. Tel/fax: +86-13778082737. E-mail address: yuchunmei@swust.edu.cn.

1. Introduction

The lithium-ion battery has recently become the most promising power battery because of the manufacturing technology improvement, which plays an important role in its power supply application. The lithium-ion battery pack has been introduced into a large number of applications, such as: hybrid buses, pure EVs, underwater weapons, underwater vehicles, as well as the aerospace [1, 2]. However, the safety of the lithium-ion battery pack is still an issue attracting great attention, which affects the utilization efficiency of its capacity and life directly, leading to accidents in several cases [3]. For the entire lifespan, the key parameter named as State of Charge (SOC) has a great influence on its power supply effect [4]. Therefore, the real-time working state monitoring assesses the overall working performance.

The core factor SOC in the Battery Management System (BMS) is quite important to the battery-based energy storage and supply systems in various working conditions [5]. With respect to the cell-to-cell battery difference, the technology design of the associated BMS equipment becomes more and more challenging [6], which should be investigated under the limited computational resource requirement conditions [7]. The SOC value is necessary to be estimated accurately by the BMS for the power application battery packs [8]. However, the technical bottleneck of the accurate SOC estimation is rather difficult to be solved [9], due to the immature management of the associated BMS equipment. It is used for the energy supply, which has stability and reliability requirements [10], aiming to avoid over-discharge and over-charge risks by conducting the battery situation treatments.

The capacity and SOC of the lithium-ion battery packs are changing along with the electro-chemical degradation process [10]. These changes are difficult to be measured online directly [11] in the aircraft power supply system, but it should be known for a certain accurate degree to monitor the energy state in real time [12]. Without the working state estimation and the energy adjustment that should be carried out by the associated BMS equipment, the aircraft will be confronted with the emergency energy loss and safety out of control issues [13]. The high energy density is the important basis of the performance indicator choice [14]. The working state estimation can be realized by using different modeling algorithms [15, 16] for the lithium-ion batteries, in which the Coulombic efficiency should be also considered [16]. The $LiCoO_2$ is used as the lithium-ion battery pack of the aerial emergency power supply, which consists of multiple series-connected battery cells, heating components, sampling resistors, temperature sensors, and sockets. The topology structure of the aircraft power system is shown in Fig. 1.

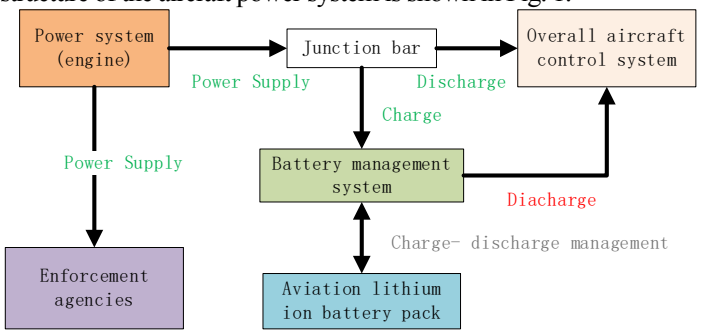

Fig. 1.The structure of the aircraft power system

Due to the necessity and urgency requirements of finding reliable SOC monitoring methods, a novel approach based on the adaptive Kalman Filter (KF) algorithm was proposed [17] by using the strong tracking cubature. The discharging and charging pattern of the lithium-ion battery was also studied by using the improved Extended Kalman Filter (EKF) algorithm [18]. The multi-dimensional construction was also reported by the equivalent circuit modelling treatment [19] of the large-scale batteries implemented by the bilinear interpolation method. The mathematical treatment of the SOC estimation method was stated [20] for the lithium-ion batteries by the detailed interaction deduction of the standard KF and the Unscented KF together with the support vector machine

algorithm. A naive Bayes model is constructed [21] for the robust life prediction of the lithium-ion batteries. However, the working state monitoring still lacks of systematic estimation methods [22]. The remaining capacity was also investigated [23] and the SOC estimation model was constructed [24]. The computational model was reported [25] with SOC dependencies, in which the impedance was also a core parameter to be considered [26]. The SOC estimation methods were stated [27] as well as the Ampere-hour (Ah) counting method [28]. A data-driven modeling method is proposed [29] for the EV applications and the real-time SOC estimation is also realized [30]. The particle model was implied [31] together with the predictor-corrector strategy [32].

The SOC estimation is challenging and requires accurate online estimation performance [33], which is embedded in the BMS of the power lithium-ion battery packs [34]. The SOC estimation can be realized by considering the consistency evaluation, which is named as State of Balance (SOB). The deterministic battery Equivalent Circuit Model (ECM) was used for the high safety requirement of the power lithium-ion battery pack, aiming to avoid its malfunction. Meanwhile, it is quite necessary to track the SOC estimation and the output voltage errors. As a result, the adaptive estimation algorithm named as Unscented Kalman Filter (UKF) was also used in the correction treatment together with the self-learning adaptation analysis, proposing a reliable energy state monitoring and management method for the power lithium-ion battery packs. The aging information is quite important to realize the accurate SOC estimation, which should be used in the effective energy management process, even if no direct aging sources can be gained from the iterative calculation process. As can be known from the actual working conditions, the aging information can be characterized by two parts of the long-term and short-term effects. The long-term influence comes from the long accumulation of cycling charge-discharge application, which can be characterized by using the OCV-SOC relationship curve. Meanwhile, the short-term influence can be described by the real-time cycling number record. As a result, the main factors can be identified and established, which are realized by using the Optimized Operation Strategy (OOS).

A novel comprehensive method is proposed to realize the SOC estimation of the lithium-ion battery pack, in which the correction treatment of SOB and aging process are investigated. Then, the estimation model is conducted by using the improved UKF and the improved variation coefficient is introduced to evaluate the cell-to-cell consistency in the battery pack. The mathematical method of the instruction and principle is analyzed, which is followed by the description of the BMS and Battery Maintenance and Testing System (BMTS) that are designed and implemented to realize the working state monitoring purpose.

2. Mathematical analysis

The iterative SOC calculation process is provided for the power lithium-ion battery packs, in which the Lithium-ion cobalt oxide batteries are used because of the good security reliability of the aircraft power supply domains. The proposed method is realized by the improved UKF algorithm combined with the discharge and charge experimental treatment process.

2.1. Working principle analysis

The internal working state monitoring is quite important to be embedded in the associated BMS equipment, including the SOC estimation model that is built for the application feature description [35]. The power supply ability evaluation named as State of Health (SOH) is mainly composed by the State of Life (SOL) and fault limits, in which the core estimation factors are considered. The fault diagnosis consists of sensors, actors, network, and other relative parameters [36]. The estimation process of the main factor SOC can be investigated by considering the zero load voltage named as Open Circuit Voltage (OCV) [37]. The Ah segmentation method is also used in the SOC estimation process of the power lithium-ion batteries [38]. The KF-based methods can realize the online parameter identification and correction in the iterate SOC calculation process, which is applied to the working state monitoring of the power lithium-ion battery packs that are settled in various working conditions [39]. The parameter named as State of Function (SOF) is also utilized in the associated BMS equipment, according to which the battery packs are maintained [40].

The single battery cell is supposed to comprise the positive electrode, separator and negative electrode. The organic solvent electrolyte is a carbonate [41] and the overall dimension of the battery case is steel and square. Its overall reaction together with the cathode and negative electrode reactions are shown in Equation 1 respectively.

$$\begin{cases} \mathrm{P}: \ LiCoO_2 \underset{\mathrm{d}}{\overset{\mathrm{c}}{\rightleftharpoons}} Li_{1-x}CoO_2 + xLi + xe^- \\ \mathrm{N}: xLi + xe^- + 6C \underset{\mathrm{d}}{\overset{\mathrm{c}}{\rightleftharpoons}} Li_xC_6 \\ \mathrm{T}: LiCoO_2 + 6C \underset{\mathrm{d}}{\overset{\mathrm{c}}{\rightleftharpoons}} Li_{1-x}CoO_2 + Li_xC_6 \end{cases} \quad (1)$$

Wherein, the physical meaning of symbols are shown as follows: P (Positive), N (Negative), T (Total reaction), c(charge), and d(discharge). The lithium-ion battery pack using the $LiCoO_2$ has attracted a lot of interest due to its obvious advantages, which is also used as the main emergency energy source of the aircraft. The intelligent SOC calculation algorithm makes its value to be estimated accurately, which can be used for the working state monitoring.

2.2. Equivalent circuit model construction

The battery ECM modeling technique can be translated into the state-space differential equations in the working state estimation process [42], the parameter identification of which cannot be realized in real time and directly in the associated BMS equipment [43]. However, the dynamic performance parameters can be captured in its power supply systems with electrical circuit elements [44]. The proposed ECM modeling method can be investigated by using the electro-chemical parameters.

The model-based SOC estimation method has been previously developed [45]. There are some cell-to-cell variations on voltage, capacity and temperature, which will be serious along with the battery aging process [46]. The energy storage and power delivering ability should be known for the reliable energy supply and safety protection against the lithium-ion battery packs. By the ECM modeling analysis, the state-space equation can be obtained and it is shown in Equation 2.

$$U_L = U_{OC} - C_b\left(\int I_L dt\right) - R_O I_L - R_p I_p \quad (2)$$

The power lithium-ion battery pack can be applied to the high power energy supply application, in which the SOC-based energy control adjustment should be conducted by the associated BMS equipment. As a result, the parameter relationship function of the observation and state variables at different sampling time points can be obtained as shown in Equation 3.

$$\begin{bmatrix} U_{OC} \\ C_b \\ R_O \\ R_P \end{bmatrix} = \begin{bmatrix} 1 & \int_0^a I_{L,a}dt & I_{L,a} & I_{P,a} \\ 1 & \int_0^b I_{L,b}dt & I_{L,b} & I_{P,b} \\ 1 & \int_0^c I_{L,c}dt & I_{L,c} & I_{P,c} \\ 1 & \int_0^d I_{L,d}dt & I_{L,d} & I_{P,d} \end{bmatrix} \begin{bmatrix} U_{L,a} \\ U_{L,b} \\ U_{L,c} \\ U_{L,d} \end{bmatrix} \tag{3}$$

Wherein, U_{OC} is used to characterize the OCV value and C_b represents the line equivalent capacitance. I_L is the current in the circuit loop. The parameters of *a*, *b*, *c* and *d* are the sampling time points respectively, which are used to characterize the different time-point working states. The curve fitting results and experimental data points can be obtained for the OCV values towards the varying SOC level by the Hybrid Pulse Power Characteristic (HPPC) test. Furthermore, the battery parameters are obtained by using the accurate ECM battery model, according to which a recursive solution of the SOC estimation can be provided by using the KF-based algorithms together with the nonlinear treatment of the state parameters. Meanwhile, the SOC estimation parameter vector changes relatively fast along with the time variation, in which the ECM construction and iterate calculation can be realized in the dynamic SOC estimation category.

2.3. Comprehensive estimation treatment

The SOC is an important aspect in the associated BMS equipment that should be estimated real-timely, which is usually used to describe the core battery parameter and the aging performance [47]. In order to realize the real-time SOC estimation accurately, an online calculation and correction method is proposed and realized. The sampling data point selection is based on the Unscented Transform (UT) processing treatment [48], the state-space description of which is combined with the prior mean and the variance values. The $2n$+1 Sigma dataset and its weight coefficients are obtained through the following UT treatment. The statistical SOC characteristics can be expressed by using the Equation 4.

$$\begin{cases} SOC^{(i)} = \overline{SOC}, i = 0 \\ SOC^{(i)} = \overline{SOC} + \left(\sqrt{(n+\lambda)P}\right)_i, i = 1, \cdots, n \\ SOC^{(i)} = \overline{SOC} - \left(\sqrt{(n+\lambda)P}\right)_i, i = n+1, \cdots, 2n \end{cases} \tag{4}$$

Wherein, *i* is the serial number of the sample data sequence and *P* is its covariance matrix. The variance *P* is the square root product of the arithmetic square root that is shown in Equation 5.

$$\left(\sqrt{P}\right)^T \left(\sqrt{P}\right) = P \tag{5}$$

The iterative UT calculation process is achieved by using the following steps: First of all, the data points of the power lithium-ion battery pack can be obtained according to the original SOC distribution screening of the state value. Then, these selected sampling data points should be substituted for the state and observing equations. Furthermore, the data points of the nonlinear equations are analyzed to obtain the expected SOC values. The SOC estimation accuracy reaches the second order by this treatment, which is higher than the accuracy of the EKF-based estimation method that can be acquired by using the Taylor series expansion.

The corresponding weights of these sampling data points are calculated, in which the weighting coefficient and the sample data sequence can be obtained by the weighted value calculation process that is shown in Equation 6.

$$\begin{cases} \omega_m^{(0)} = \dfrac{\lambda}{n+\lambda}, \lambda = \alpha^2\left(n+\kappa\right) - n \\ \omega_c^{(0)} = \dfrac{\lambda}{n+\lambda} + \left(1 - \alpha^2 + \beta\right) \\ \omega_m^{(i)} = \omega_c^{(i)} = \dfrac{1}{2\left(n+\lambda\right)}, i = 1, \cdots, 2n \end{cases} \tag{6}$$

Wherein, the subscript *m* represents the mean value of the Sigma data point set of the SOC. The subscript *c* can be used to describe the covariance, which characterizes the variance in the Sigma data point set for the SOC. The superscript *i* can be used to represent the serial number of sampling data points. λ is the overall scaling factor, which is used to describe the scaling characteristics and reduce the SOC estimation error. The choice of α determines the state distribution of the SOC value sequence. Furthermore, the parameter value of κ can be obtained by using the premise that $(n+\lambda)*P$ is a positive semi-definite matrix. By the selection of the non-negative weight coefficient β, the statistical high-order term error of the state-space equation is incorporated to ensure that the high-order term influence is covered in the UT treatment.

The data points numbered as $2n$+1 should be selected in the UT process, in which fewer data points in the UT process will be advantageous to the integrated BMS applications. Incorporating the conversion to the SOC estimation process, only $2n$+1=3 data points are required, in which *n* is set to be 1. The initialization weight coefficient W_0 is previously assigned to the *n*-dimensional nonlinear treatment process. The selection result of which only affects the fourth-order and higher order Sigma data point set. The remaining weight coefficients can be selected from W_1 to W_n. The first three-element vector of *SOC* from 0 to 2 can be obtained according to the weight coefficient W_1, and the required n+2 data point set sequences are generated with *n*-dimensional features, so that the vector is calculated recursively. The UT treatment can be implemented, which is used in the parameter preprocessing calculation steps. The iterative calculation process of the real-time SOC estimation is shown in Fig. 2.

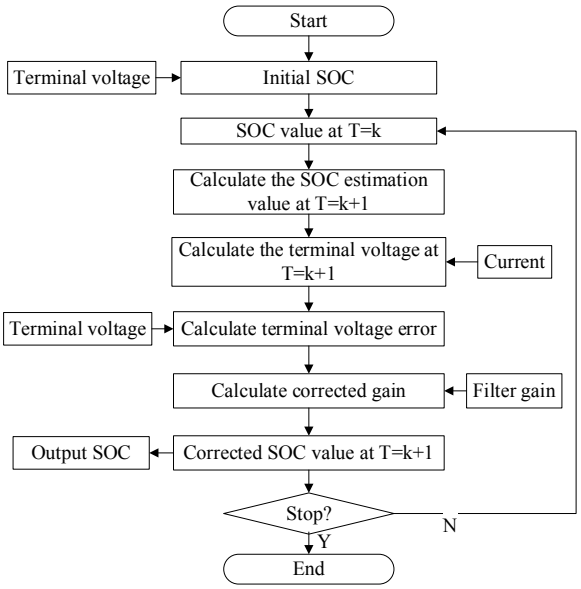

Fig. 2.The iterative SOC estimation process

The iterate calculation process includes the random state variable SOC fused with Gaussian white noise $w(k)$. Meanwhile, an observation random variable $U_L(k)$ is fused with the Gaussian white noise $v(k)$. $f(*)$ is the nonlinear state equation in the SOC estimation process and $g(*)$ is the nonlinear observation equation that describes the characteristics of the output Closed-Circuit Voltage (CCV). The process noise variance matrix $w(k)$ and the observed noise matrix $v(k)$ can be described by using Q and R. The SOC estimation calculation treatment of different time point k is realized by using the following steps.

S1: The Sigma data sequence can be constructed by using a series of sampling points, and the corresponding weight coefficients can be obtained by conducting the UT treatment that is shown in Equation 7.

$$SOC^{(i)}(k\text{-}1)=\begin{bmatrix} SOC(k\text{-}1) \\ SOC(k\text{-}1)+\sqrt{(n+\lambda)P(k\text{-}1)} \\ SOC(k\text{-}1)-\sqrt{(n+\lambda)P(k\text{-}1)} \end{bmatrix} \tag{7}$$

S2: A detailed methodology is used to assess the SOC value, in which the electrical topology and balancing adjustment control has been conducted in our previous research. The one-order prediction of the sinusoidal $2n$+1 data point sequence can be calculated as shown in Equation 8.

$$SOC^{(i)}(k\,|\,k\text{-}1)=f\left[k,SOC^{(i)}(k\text{-}1)\right],i=1,2,\cdots,2n+1 \tag{8}$$

S3: The one-step prediction of the state-space SOC distribution and its variance matrix can be calculated. The weighted perform summation of the Sigma data pointed sequence and the SOC estimation can be implemented in combination with the various calculation expressions of the UT processing treatment. The algorithm uses the last time-point corrected SOC values by using the mathematical description of the state-space function to replace the real-time calculated SOC value. According to this calculation treatment, only one step calculation is needed to obtain the predicted SOC value. The prediction process is implemented by the settled three data points, and the average value can be calculated by combining the weighting coefficients that are shown in Equation 9.

$$SOC(k\,|\,k\text{-}1)=\sum_{i=0}^{2n}\omega^{(i)}SOC^{(i)}(k\,|\,k\text{-}1) \tag{9}$$

Then, the predicted SOC variance value can be obtained as shown in Equation 10.

$$P(k\,|\,k\text{-}1)=\sum_{i=0}^{2n}\omega^{(i)}\left[SOC(k\,|\,k\text{-}1)-SOC^{(i)}(k\,|\,k\text{-}1)\right]*\left[SOC(k\,|\,k\text{-}1)-SOC^{(i)}(k\,|\,k\text{-}1)\right]^{T}+Q \tag{10}$$

S4: A new sequence of Sigma data points can be obtained by applying the step-less UT treatment process once again to the one-step prediction value that is shown in Equation 11.

$$SOC^{(i)}(k\,|\,k-1)=\begin{bmatrix} SOC(k\,|\,k-1) \\ SOC(k\,|\,k-1)+\sqrt{(n+\lambda)P(k\,|\,k-1)} \\ SOC(k\,|\,k-1)-\sqrt{(n+\lambda)P(k\,|\,k-1)} \end{bmatrix} \tag{11}$$

S5: The iterate calculation of the CCV value is presented as follows. Firstly, the timely updated calculation in the prediction step is conducted with the initial estimation value of the state parameter SOC and its error covariance. The Sigma data point sequence can be obtained in the previous step, which is substituted for the observation equation, obtaining the predicted observed variable matrix that is shown in Equation 12.

$$U_L^{(i)}(k\,|\,k-1)=h\left[SOC^{(i)}(k\,|\,k-1)\right],i=1,2,\cdots,2n+1 \tag{12}$$

The inaccurate online SOC estimation is the main drawback in the commercialization process of the lithium-ion battery packs. The characteristics of which limit the endurance mileage of the power supply application for different working conditions. Moreover, the associated BMS equipment including the accurate SOC estimation requires high calculation resource requirement to prevent manufacturers from applying battery packs.

S6: The predicted CCV value of the output circuit can be calculated, which can be used as the autocorrelation and cross-correlation matrices. The calculation of these values can be realized by the weighted summation of the predicted values of the Sigma data point sequence.

(1) The forecasted mean value is shown in Equation 13.

$$\overline{U}_L(k\,|\,k\text{-}1)=\sum_{i=0}^{2n}\omega^{(i)}U_L^{(i)}(k\,|\,k\text{-}1) \tag{13}$$

(2) The measurement correction is updated at the same time, in which the autocorrelation matrix is realized by Equation 14.

$$P_{U_L(k)U_L(k)}=\sum_{i=0}^{2n}\omega^{(i)}\left[U_L^{(i)}(k\,|\,k\text{-}1)-\overline{U}_L(k\,|\,k\text{-}1)\right]\left[U_L^{(i)}(k\,|\,k\text{-}1)-\overline{U}_L(k\,|\,k\text{-}1)\right]^{T}+R \tag{14}$$

(3) The cross correlation matrix is realized by using Equation 15.

$$P_{SOC(k)U_L(k)}=\sum_{i=0}^{2n}\omega^{(i)}\left[U_L^{(i)}(k\,|\,k\text{-}1)-\overline{U}_L(k\,|\,k\text{-}1)\right]\left[U_L^{(i)}(k\,|\,k\text{-}1)-\overline{U}_L(k\,|\,k\text{-}1)\right]^{T} \tag{15}$$

S7: The Kalman gain matrix can be obtained by the iterate calculation that is shown in Equation 16.

$$K(k)=P_{SOC(k)U_L(k)}P_{U_L(k)U_L(k)}^{-1} \tag{16}$$

S8: The state and error-covariance update processing can be implemented in the following two steps along with the non-linear characteristics.

(1) The state-updating process can be conducted by the calculation treatment that is shown in Equation 17.

$$SOC(k)=SOC(k\,|\,k\text{-}1)+K(k)\left[U_L(k)-U_L(k\,|\,k\text{-}1)\right] \tag{17}$$

(2) The error update treatment is calculated by Equation 18.

$$P(k)=P(k\,|\,k\text{-}1)-K(k)P_{U_L(k)U_L(k)}K^{T}(k) \tag{18}$$

The iterate calculation framework is constructed in order to realize the iterative SOC estimation process. In the one-step SOC prediction calculation process, the non-linear conversion problem of the mean and variance in the SOC estimation can be solved by using the reduced three-point UT treatment. The sampling data sequence is set for the approximate posterior in the SOC estimation process, which is conducted without performing the Jacobian matrix. There is no a high-order term ignoring the problem with the calculation process, which makes the statistical features having a high accuracy advantage, reducing the nonlinear errors effectively. The weighted Sigma data points are implied by streamlining these three particles, and the mean value of the detected data samples can be calculated and taken as the predicted value accordingly. In this way, the SOC estimation model can be built by the UT processing and the improved UKF algorithm. The detailed conducting process is shown in Fig. 3.

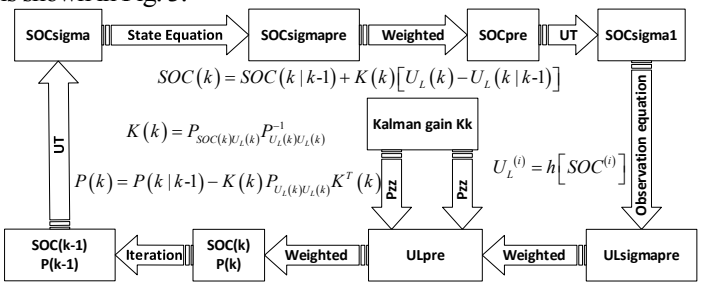

Fig. 3. The detailed SOC computation process

The electrolyte and charge-transfer resistances are adopted as the inputs, according to which the SOC values are predicted to compute the corresponding battery capacity. As stated above, the comprehensive calculation should be suitable for the high energy and power specification of the lithium-ion battery packs. Therefore, a large number of input parameters are related to the working environments, which should be considered in the adaptive SOC estimation model design. The comprehensive SOC estimation is cast in the iterative calculation process, in which the structural analysis model is built to suit the multi-input condition characteristics. During the different step calculation of the temperature, voltage and current, the SOC estimation model is built for the comprehensive evaluation of the combined multiple input-parameters with conjunctive relations.

2.4. State of balance evaluation

The diaphragm microspore changes and other internal parameters in the lithium-ion battery packs cannot be measured directly. The Ohm resistance, polarization resistance-capacitance and other parameters also need to be measured indirectly by conducting the off-line experiments. The online measurements are only suitable and available externally for the parameters of voltage, current and temperature. As a result, the online State of Balance (SOB) evaluation can only be realized by using these parameters. In order to realize the equilibrium state evaluation among the internal connected battery cells, the numerical description and evaluation thought is investigated by the SOB calibration treatment. The SOC correction process can be improved by the model parameters and weighted factors, which is the most direct and effective way to evaluate the overall equilibrium state by detecting the voltage in real-time. The voltage detection has real-time, fast and easy implement advantages in the realization process of the online SOB evaluation. The individual cell voltage U_c is used to evaluate the SOB value of the battery pack, which can be obtained by Equation 19.

$$E(U_c)=\overline{U_c}=\frac{1}{n}\sum_{i=1}^{n}U_{ci} \tag{19}$$

In the above expression, U_{ci} is the i-th battery cell voltage in the lithium-ion battery pack, and n is the total battery cell number. The calculation result $E(U_c)$ represents the expected voltage value of all inter-connected battery cells, which is the average of the voltage value. The standard deviation parameter δ is an important technical indicator of the differential working state evaluation. Therefore, the proposed SOB evaluation method adopts the measurement of the standard deviation and probability distribution. Then, the SOB together with its quantitative evaluation index is applied to the SOC estimation, meeting the post-quantification equilibrium evaluation target. As a result, the inconsistent equilibrium parameter SOB is investigated and its dispersion degree is defined by the probability statistics theory. The mathematical description of which is shown in Equation 20.

$$\delta^2=\frac{1}{n}\sum_{i=1}^{n}\left(U_{ci}-E(U_c)\right) \tag{20}$$

δ^2 is used to characterize the fluctuation of the voltage values (U_{c1}, U_{c2}, ..., U_{cn}) of all the internal connected battery cells, and then the cell voltage inconsistency can be described. Meanwhile, the variation coefficient θ can describe the influence extent of voltage fluctuation more accurately according to the differential degree evaluation target. The calculation process of which is shown in Equation 21.

$$\theta=\frac{\delta}{E(U_c)}=\sqrt{\frac{1}{n}\sum_{i=1}^{n}\left(\frac{U_{ci}-E(U_c)}{E(U_c)}\right)^2} \tag{21}$$

In the above expression, δ^2 is used to denote the voltage difference variance in the internal battery cells of the lithium-ion battery pack. Furthermore, the above evaluation parameters can be obtained by using the average voltage value $E(U_c)$ among the respective battery cells through the voltage value detection of each single cell, which can describe the average level of each single battery voltage. The voltage standard deviation δ describes the various discrete degree of the battery cell voltage.

When the standard deviation of each cell voltage decreases, the voltage deviation from each battery cell will be smaller accordingly together with the cell-to-cell consistency improvement. In the above calculation process, the variance describes the operating voltage distribution of all the battery cells. The variation coefficient is a representation of the single-cell voltage observation variability. Through the introduction to this parameter, the consistency state under different working conditions can be described. The calculation of the parameter θ needs to be carried out with the square root treatment. Finally, the squared parameter ε is used as the variation coefficient is employed to evaluate the equilibrium state, and its calculation process is shown in Equation 22.

$$SOB=\varepsilon=\theta^2=\frac{1}{n}\sum_{i=1}^{n}\left(\frac{U_{ci}-E(U_c)}{E(U_c)}\right)^2 \tag{22}$$

In the above expression, ε describes the battery cell voltage inconsistency, in which θ is employed to define the voltage

variation coefficient of the battery cells. In order to realize the dynamic equilibrium state evaluation, the real-time sampling and calculation of the individual cell voltages should be investigated. The mathematical difference description of the single battery cells can be provided, which offers a quantifiable parameter index for the equilibrium state evaluation. During the calculation process, the difference is described to characterize the correlation between the interconnected individual battery cells in the entire lithium-ion battery pack. The equivalent electromotive force and the resistance parameter under the equilibrium state influence are obtained and expressed in the equivalent model. The voltage change under the influence of the equilibrium state ε can be investigated, according to which the calculation expression can be obtained by Equation 23.

$$\begin{cases} U_\delta(k)=\varepsilon * U_{OC}(k)=\dfrac{1}{n}\sum\limits_{i=1}^{n}\left(\dfrac{U_{ci}(k)-E(U_c(k))}{E(U_c(k))}\right)^2 * U_{OC}(k) \\ R_\delta(k)=\varepsilon * R_o(k)=\dfrac{1}{n}\sum\limits_{i=1}^{n}\left(\dfrac{U_{ci}(k)-E(U_c(k))}{E(U_c(k))}\right)^2 * R_o(k) \end{cases} \tag{23}$$

The main parameter which determines the problem should be solved in the SOB calculation process of the battery cells, according to which the interaction relationship of the group working characteristic is analyzed and taken as the main basis of the correction process. By conducting the integrated SOB evaluation of the battery cell voltages, the numerical and mathematical SOB description is carried out in the evaluation process. In the SOB assessment framework, the index system is established and the influencing factors are determined according to the model factor analysis, in which the SOB evaluation of the internal connected battery cells and their calculation influence should be considered.

The SOC level information about the battery cell is necessary for the working state monitoring, which is built in the associated BMS equipment with the solution design by using series and parallel topologies. As a result, this thought is practical for the high power packing energy supply applications, in which the comprehensive credibility should be established for these various input parameters.

2.5. Aging process impact correction

Through the mathematical SOC estimation study method, the KF-based algorithm is introduced into the iterative calculation process. Furthermore, it is realized by combining the model parameter identification. By the SOC estimation method research in the aerial application environment and the experimental analysis of the charging and discharging process, the estimation process is realized and the structural model is constructed. The iterative calculation process is combined with the model parameter identification. Experiments are carried out by the standard $1C_5A$ discharge capacity together with the Ah integral method, in which the actual released power state Q_{n_Deter} can be obtained. The parameter can be characterized by using the end-time-point SOC value of the intermittent discharge period, which is described by using the symbol SOC_n. The relative SOC change ratio can be obtained as shown in Equation 24.

$$\delta_{SOC}=\frac{SOC_n}{SOC_0}\times 100\% \tag{24}$$

The balancing charge mode is used to make the lithium-ion battery pack to be fully charged, according to which the initial SOC replacement can be investigated. In this case, the amount of SOC change is represented by the normalization of Q_n. The influence coefficient K_Q of the aging state on the electric quantity of Q_n can be obtained and the calculation expression is shown in Equation 25.

$$K_Q=\delta_{SOC}=\frac{SOC_n}{SOC_0}\times 100\%=\frac{Q_{n\_Deter}}{Q_{0\_Rated}}\times 100\% \tag{25}$$

Because of the slow change aging process characteristics of the lithium-ion battery pack, the retrieval of the functional relationship can be achieved by the regular calibration. By the synchronous acquisition and correction of the relative values of the rated capacity and the cyclic discharge-charge number, the correcting calculation formula for the overlapping cyclic number can be obtained as shown in Equation 26.

$$\Delta Q_n=f(N) \tag{26}$$

Wherein, N is the cycling discharge-charge number after the last capacity measurement and ΔQ_n is the subsequent cycling effect on the rated capacity Q_n. The mathematical aging process description of the rated capacity can be obtained as shown in Equation 27.

$$Q_n=K_Q * Q_{n\_Rated}-\Delta Q_n \tag{27}$$

The characteristics are analyzed in the experiments, in which the capacity aging law can be obtained by recording the discharging capacity of every cycling discharge and charge process. When the material structure is changed along with the cyclic discharge-charge number, the lithium-ion battery pack will also experience the mathematical characteristic behavior change. As a result, there is an obvious correlation between the capacity aging characteristic and the cycling number. Therefore, it is necessary to characterize the discharging and charging performance. The test data analysis and mining performance can be conducted accordingly, in which the capacity aging characteristics are obtained.

There is a significant linear attenuation relationship between the capacity and the cycling discharge-charge number. Therefore, the correction processing is performed by using the aging influence coefficient, in which the cycling number of charging and discharging treatment is considered. Furthermore, the charge and discharge performance of the SOC estimation process of the aircraft lithium-ion battery pack is characterized as shown in Equation 28.

$$R\_C=f(N)=p_1 * N+p_2 \tag{28}$$

The normalized capacity change can be expressed towards the number of the charging and discharging cycles. p_1 is the coefficient of the first order and p_2 is the constant term. By conducting the linear fitting treatment, the value of the first term is obtained as p_1 = -0.0001029, and the value of the constant term is p_2 = 1.0000. Therefore, the attenuation rate of the rated capacity per cycle is p_1, and the real-time correction of the capacity is obtained as shown in Equation 29.

$$Q_n=K_Q * Q_{n\_Rated}-\Delta Q_n=\left(K_Q+p_1 * N\right) * Q_{n\_Rated} \tag{29}$$

The battery capacity can be treated as a constant variable for a certain time period and the variation law should be used in the real-time SOC estimation process. Meanwhile, as the battery capacity aging law can be obtained by the cycling discharge-charge experiments, it is quite necessary to extract the accurate battery capacity aging characteristic description. As a result, the aging factor is used to express the application characteristics, providing great supports for the accurate SOC estimation. The proposed comprehensive SOC estimation method is realized in the associated

BMS equipment by using the iterative calculation and correction process, which can be conducted accordingly by the modeling establishment of the multiple-input parameter condition in the power supply system.

3. Experimental analysis

The associated BMS equipment together with the SOC assessment model is designed and built, according to which the verification is conducted by the experimental discharge-charge process together with the Battery Maintenance and Test System (BMTS) platform. The maintenance cabinet system of the BMTS platform is designed by using the RS485 field-bus. The electronic loads are embedded into the BMTS platform to simulate the energy consumption process of the loading sub-systems in the aircraft. The data acquisition and record subsystems are used to record the core parameter values, which is also used for the energy management of the on-chip BMS equipment in the computing realization process. The high accuracy current sensors are used in the BMTS platform, the accuracy of which is 0.10%. The C# type program is done in the Industrial Personal Computer (IPC), which is designed and used as the human-computer interaction interface. Aiming to satisfy the comparative data processing and real-time monitoring process requirement, the microcontroller STM32 is used in the associated BMS equipment. The overall structure of the BMTS platform is shown in Fig. 4.

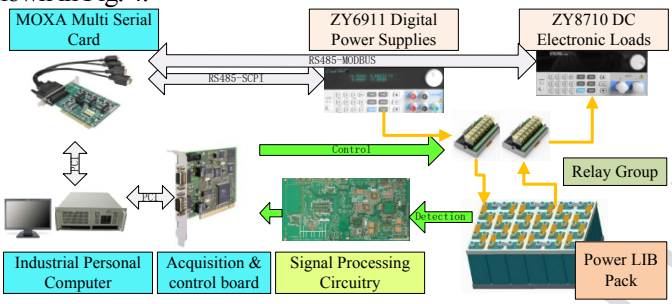

Fig. 4.BMTS equipment for the battery pack

The high-accuracy detection sub-system is emoting for the core parameter measurement, and the signal data onto the KF-based SOC estimation is conducted by the mathematical calculation treatment process. According to the online application functionality and the performance requirements, the working state detection and analysis sub-system is designed and embedded in the associated BMS equipment, which constructs the SOC assessment. There are 14 digital powers used for the balancing charge treatment of the BMTS platform, together with two big powers from Taiwan for the serial charging process.

3.1. Charge-discharge working characteristics

The ability to store and release energy is affected by the internal interconnected battery cells in the lithium-ion battery packs. Therefore, the SOC of the lithium-ion battery pack is determined by the performance of each individual battery cell. In the cycling charge-discharge experimental process, the aerial lithium-ion battery pack samples are selected and the experimental test of the cycling charge-discharge maintenance should be conducted. The total voltage, current and each cell voltage data are detected in real-time along with the variation rule analysis of each parameter. During the cycling charge and discharge test, the conditions of each parameter are set to avoid over-charge or over-discharge for the safety protection of the lithium-ion battery pack.

The aerial lithium-ion battery pack is selected as the experimental samples, in which 7 cells are connected serially. The constant-current and equalization charging treatment is conducted, in which the threshold CCV value is set to be 28.840V during the charging process. In the equalization charging process, the voltage conversion condition of constant-current charging and constant voltage charging of each unit is 4.150V. The stopping condition of the equalizing charging constant voltage replenishing electric power is less than or equal to 2.000A, avoiding the over-charge phenomenon in the case of fully capacity utilization of each battery cell. During the discharge process, the discharge stop condition is set when the CCV voltage is less than or equal to 21.000 V or the voltage of any battery cell is 3.000 V or less. In this way, the occurrence of over-discharge is avoided in the case of improving the capacity utilization efficiency of the lithium-ion battery pack. Under the premise of ensuring its safety, the experimental study of charge-discharge cycles can be carried out, in which the working characteristic variation on the lithium-ion battery pack is analyzed under different SOC conditions. Through the analysis of the group working characteristics, the data basis of the equivalent model construction can be provided for the lithium-ion battery pack, and the working characteristics of the lithium-ion battery pack are more accurately characterized. Furthermore, the SOC estimation accuracy of the lithium-ion battery pack can be improved by these experimental analysis results. During the cycling charge and discharge process of lithium-ion battery packs, the CCV has a certain regularity with time, which has obvious pointed inflection characteristics. The variation characteristics of the lithium-ion battery pack are shown in Fig. 5.

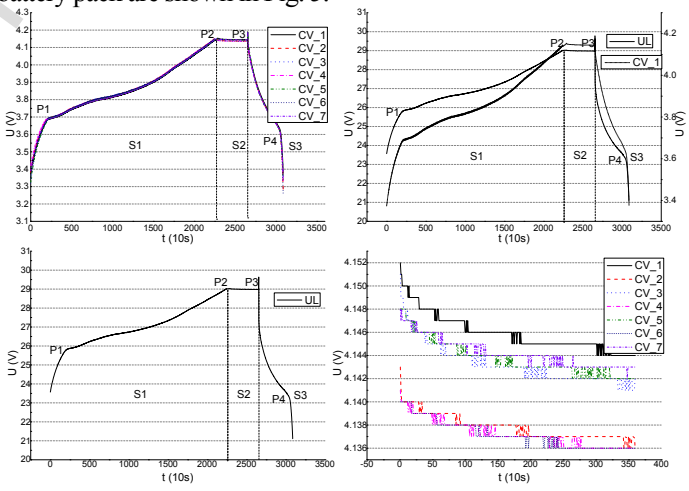

Fig. 5.Cycling charge-discharge working characteristics

As can be seen from the experimental results, the charging process can be divided into four different stages by the three points of P1, P2 and P3. The small current pre-charging, constant-current fast charging and constant-voltage variable current charging process can be realized according to this. The description of the supplementary power and shelving process is carried out by comparing and analyzing the CCV of the lithium-ion battery pack by conducting the equivalent voltage tracking experiment, and then the equivalent model can be improved and optimized. By extending the capacity of the individual battery cells to a group level definition, the group

capacity can be obtained by the Ah integration, which is achieved by discharging all cells in the battery pack in case of one single battery cell in the group is fully charged. As a result, the fully charged state of the whole battery pack can be achieved.

During the discharge process, the large current discharge treatment is realized by using the rapid discharge current of $1C_5A$. During the cycling charge-discharge process of the lithium-ion battery pack, the voltage variation on each internal battery cell is obtained by detecting and recording the voltage of each cell in real-time. On the basis of the variation law of each cell voltage in the group working mode, the working state of each battery cell is monitored synchronously and the safety protection is also investigated. The raw data onto the SOB evaluation among the battery cells in the lithium-ion battery pack is provided, which is used for the correction step of the SOC estimation to improve its accuracy and reliability.

3.2. SOC tracking effect under complex conditions

To verify the joint estimation applicability of the proposed SOC estimation method, the Minimum Mean Square Error (MMSE) is investigated for the SOC estimation effect evaluation purpose. The serially connected battery packs are introduced into the experiments. The estimation effect is analyzed when the SOC initial value is set to be 1, in which the experiments are conducted simultaneously along with the simulated working condition process. The SOC tracking result is described in Fig. 6.

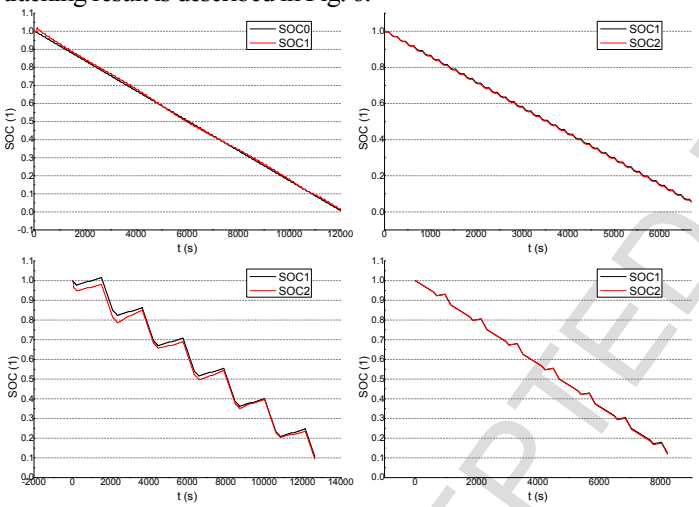

Fig. 6. SOC estimation effect analysis

As can be known from the experimental results, the proposed method shows a positive effect on the SOC estimation of the lithium-ion battery pack. Comparing with the references from [15] and [49], the SOC estimation has similar experimental values compared to the reported results, in which the average absolute error of the SOC value is only 1.83% on the proposed estimation method. According to the battery surface temperature variation along with the correctness [50], the battery diagnosis can be proved in the correction steps.

The estimated absolute error becomes small when the initial SOC value is low, which makes the estimation results to match accurately with the theoretical value. The development of the proposed correlation is involved in the experiments, in which the adaptability is analyzed by comparing the experimental data onto the actual SOC value. The least-square fitting method together with the correlation is used to establish the battery ECM model and its model parameters are calculated, in which the curve fitting treatment is conducted to identify the battery model parameters.

3.3. Noise influencing effect

The adaptability of the proposed SOC estimation method is analyzed by considering the process and observation noise influence, which is also carried out for the accuracy verification. Due to the calculating condition limitation of the processor and inevitably, the number of decimal places and the high-order terms in the calculation process is discarded. As a result, the process noise is generated, which will affect the SOC estimation results. By superposing varying process noise, the estimation effects and adaptability can be verified under different processor accuracy. The original process noise is set to be Q = 1e-10. The industrial computers and other processors have great computing ability where the process noise is small. During the analysis process of the estimating effect, the process noise is set as Q1 = 1e-10, Q2 = 1e-8, Q3 = 1e-6 and Q4 = 1e-3 respectively. By conducting the experiments, the SOC estimation results can be obtained as shown in Fig. 7.

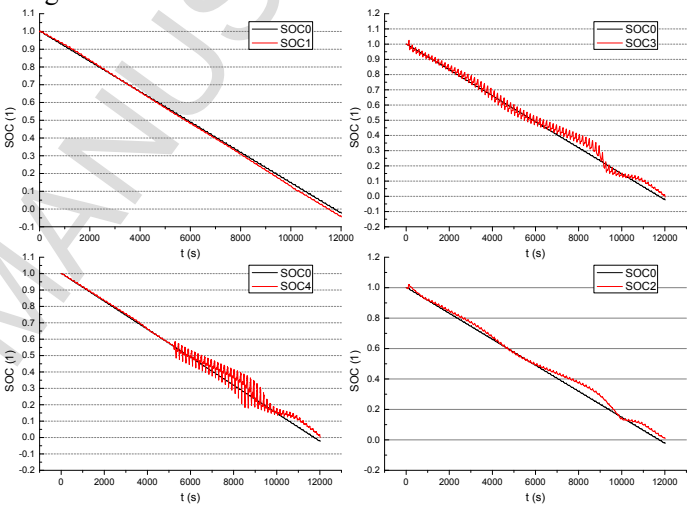

Fig. 7. The SOC estimation effect under different noise influence

In the Figure, SOC0 is obtained by the Ah integration, and SOC1 is the SOC value with Q = 1e-10. SOC2 is the SOC value with Q = 1e-8. SOC3 is the SOC value with Q = 1e-6, and SOC4 is the SOC value when Q = 1e-3. As can be known from the experimental results, the estimated SOC results adapt the theoretical value of the whole iterative calculation process along with the varying noise influence. When the SOC value ranges from 60.00% to 20.00%, the error is large because of the platform effect [51] during this time period. The process noise influence becomes prominent as the process noise turns to be large.

3.4. State of balance correction analysis

The experimental analysis of the SOB correcting effect is carried out by conducting the verification experiments. Furthermore, the SOC estimation effect can be obtained through the estimation effect analysis under various working conditions. In the SOC estimation process, the SOB influences the description of the correction effect which can be realized by adding the influence factor of the SOB into the correction step. The comparative experiments are conducted, in which the different SOC tracking results can be

obtained by the varying methods, including Ah integral, considering or not considering the SOB influence. The SOC estimation results can be obtained when the consistency situation of the lithium-ion battery pack is good, which are shown in the left part of Fig. 8. In the Figure, SOC1 is obtained by the Ah method. SOC2 signifies the SOC value considering the SOB addition treatment. SOC3 characterizes the SOC value without considering the SOB influence. As can be known from the experimental results, the correction effect of the SOB factor is small when the equilibrium condition is good. Whether or not the influence of this factor is considered, high values of SOC accuracy estimation results can be obtained in the experiments.

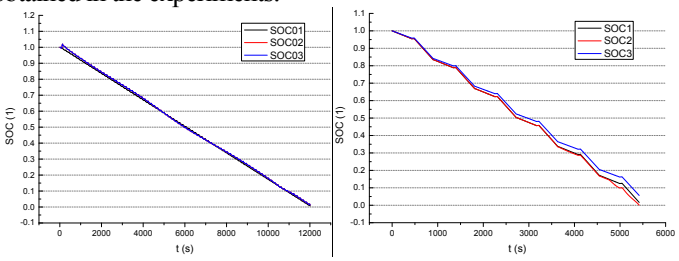

Fig. 8.Estimation effect under different SOB conditions

Furthermore, the poor balance condition is obtained by the cycling discharge-charge treatment, which is used to conduct the SOC estimation effect analysis under terrible working conditions of the lithium-ion battery pack. In the SOC estimation process, the SOB influences and the description of the correction effect can be realized by adding the influence factor of the SOB and the situation is not considered by the SOB influence. The experimental results are shown in the right part of Fig. 8. As can be known from the experimental results, the correction effect of the SOB correction factor is obvious under the condition of poor balance in the lithium-ion battery pack. The SOB impact becomes more and more obvious along with the time as a continuation of the main discharge conditions. As a result, it should be considered in the SOC correction and in the energy balancing processes [39]. The comprehensive estimation method can obtain high accuracy values of SOC ~~values~~ under complex working conditions. The estimation accuracy rate was found to be: 98.17% by using the method of the comprehensive SOC estimation strategy. This method has high precision and easy calculation advantages when it is compared with the existing reports using the KF-based algorithms [9, 31]. The related experimental studies have been done, in which the associated BMS equipment is combined with this comprehensive method.

4. Conclusion

A novel and powerful working state monitoring method is proposed, in which the SOC estimation is realized by the improved UKF-based iterative calculation model and verified by the implementation of the associated BMS equipment along with the iterative calculation. In order to characterize the cell-to-cell battery consistency, an iterative SOB evaluation method is proposed by conducting the improved variation coefficient calculation. The intermittent measurement and real-time calibration calculation process is applied to characterize the capacity change of the battery pack towards the cycling maintenance number, according to which the aging process impact correction can be realized. The comprehensive SOC estimation model is realized by using the improved UKF method, effectively guaranteeing the power supply reliability and providing a positive useful promotion role of the lithium-ion battery packs.

Acknowledgments

This research was supported by National Natural Science Foundation (No. 61801407), Sichuan Province Science and Technology Support Program (No. 2018GZ0390, 2017FZ0013), Scientific Research Fund of Sichuan Provincial Education Department (No. 17ZB0453), Doctoral fund (18zx7145), Longshan Talent Program (18lzx665), Teaching Research Project (18zx7145, 18gjzx11, 18xnsu12), Sichuan Science and Technology Innovation Cultivation Project (No. 201810619082, 201810619028, 201810619078, 201810619029). Thanks to the sponsors. CF would like to express his gratitude to RGU for its support.

References

1. Xiong, R., et al., *A Double-Scale, Particle-Filtering, Energy State Prediction Algorithm for Lithium-Ion Batteries.* Ieee Transactions on Industrial Electronics, 2018. **65**(2): p. 1526-1538.
2. Chen, X.P., et al., *Robust Adaptive Sliding-Mode Observer Using RBF Neural Network for Lithium-Ion Battery State of Charge Estimation in Electric Vehicles.* Ieee Transactions on Vehicular Technology, 2016. **65**(4): p. 1936-1947.
3. Zhu, X.H., et al., *Electrochemical impedance study of commercial LiNi0.80Co0.15Al0.05O2 electrodes as a function of state of charge and aging.* Electrochimica Acta, 2018. **287**: p. 10-20.
4. Zheng, Y.J., et al., *Investigating the error sources of the online state of charge estimation methods for lithium-ion batteries in electric vehicles.* Journal of Power Sources, 2018. **377**: p. 161-188.
5. Zheng, Y.J., et al., *State-of-charge inconsistency estimation of lithium-ion battery pack using mean-difference model and extended Kalman filter.* Journal of Power Sources, 2018. **383**: p. 50-58.
6. Zheng, L.F., et al., *Differential voltage analysis based state of charge estimation methods for lithium-ion batteries using extended Kalman filter and particle filter.* Energy, 2018. **158**: p. 1028-1037.
7. Lim, D.J., et al., *A Mixed SOC Estimation Algorithm with High Accuracy in Various Driving Patterns of EVs.* Journal of Power Electronics, 2016. **16**(1): p. 27-37.
8. Hosseinimehr, T., A. Ghosh, and F. Shahnia, *Cooperative control of battery energy storage systems in microgrids.* International Journal of Electrical Power & Energy Systems, 2017. **87**: p. 109-120.

9. Lim, K., et al., *Fading Kalman filter-based real-time state of charge estimation in LiFePO4 battery-powered electric vehicles.* Applied Energy, 2016. **169**: p. 40-48.
10. Partovibakhsh, M. and G.J. Liu, *An Adaptive Unscented Kalman Filtering Approach for Online Estimation of Model Parameters and State-of-Charge of Lithium-Ion Batteries for Autonomous Mobile Robots.* Ieee Transactions on Control Systems Technology, 2015. **23**(1): p. 357-363.
11. Zhang, Z.L., et al., *SOC Estimation of Lithium-Ion Battery Pack Considering Balancing Current.* Ieee Transactions on Power Electronics, 2018. **33**(3): p. 2216-2226.
12. Zheng, L.F., et al., *Incremental capacity analysis and differential voltage analysis based state of charge and capacity estimation for lithium-ion batteries.* Energy, 2018. **150**: p. 759-769.
13. Rahman, M.A., S. Anwar, and A. Izadian, *Electrochemical model parameter identification of a lithium-ion battery using particle swarm optimization method.* Journal of Power Sources, 2016. **307**: p. 86-97.
14. Zhang, Y.L., X.Y. Du, and M. Salman, *Battery state estimation with a self-evolving electrochemical ageing model.* International Journal of Electrical Power & Energy Systems, 2017. **85**: p. 178-189.
15. Yang, F.F., et al., *A comparative study of three model-based algorithms for estimating state-of-charge of lithium-ion batteries under a new combined dynamic loading profile.* Applied Energy, 2016. **164**: p. 387-399.
16. Zhang, W.J., et al., *An improved adaptive estimator for state-of-charge estimation of lithium-ion batteries.* Journal of Power Sources, 2018. **402**: p. 422-433.
17. Xia, B.Z., et al., *A Comparative Study of Three Improved Algorithms Based on Particle Filter Algorithms in SOC Estimation of Lithium Ion Batteries.* Energies, 2017. **10**(8).
18. Zhang, G.W., et al., *Enhancement in liberation of electrode materials derived from spent lithium-ion battery by pyrolysis.* Journal of Cleaner Production, 2018. **199**: p. 62-68.
19. Kim, J., *Discrete Wavelet Transform-Based Feature Extraction of Experimental Voltage Signal for Li-Ion Cell Consistency.* Ieee Transactions on Vehicular Technology, 2016. **65**(3): p. 1150-1161.
20. Dong, G.Z., et al., *Online state of charge estimation and open circuit voltage hysteresis modeling of LiFePO4 battery using invariant imbedding method.* Applied Energy, 2016. **162**: p. 163-171.
21. Feng, T.H., et al., *Online identification of lithium-ion battery parameters based on an improved equivalent-circuit model and its implementation on battery state-of-power prediction.* Journal of Power Sources, 2015. **281**: p. 192-203.
22. Zhang, C., et al., *Online estimation of battery equivalent circuit model parameters and state of charge using decoupled least squares technique.* Energy, 2018. **142**: p. 678-688.
23. Jung, S. and H. Jeong, *Extended Kalman Filter-Based State of Charge and State of Power Estimation Algorithm for Unmanned Aerial Vehicle Li-Po Battery Packs.* Energies, 2017. **10**(8).
24. Xie, J.L., et al., *Estimating the State-of-Charge of Lithium-Ion Batteries Using an H-Infinity Observer with Consideration of the Hysteresis Characteristic.* Journal of Power Electronics, 2016. **16**(2): p. 643-653.
25. Xu, X., Z.G. Li, and N. Chen, *A Hierarchical Model for Lithium-Ion Battery Degradation Prediction.* Ieee Transactions on Reliability, 2016. **65**(1): p. 310-325.
26. Fridholm, B., T. Wik, and M. Nilsson, *Robust recursive impedance estimation for automotive lithium-ion batteries.* Journal of Power Sources, 2016. **304**: p. 33-41.
27. Yang, J.F., et al., *Adaptive State-of-Charge Estimation Based on a Split Battery Model for Electric Vehicle Applications.* Ieee Transactions on Vehicular Technology, 2017. **66**(12): p. 10889-10898.
28. Ye, M., et al., *A double-scale and adaptive particle filter-based online parameter and state of charge estimation method for lithium-ion batteries.* Energy, 2018. **144**: p. 789-799.
29. Gong, X.Z., R. Xiong, and C.C. Mi, *A Data-Driven Bias-Correction-Method-Based Lithium-Ion Battery Modeling Approach for Electric Vehicle Applications.* Ieee Transactions on Industry Applications, 2016. **52**(2): p. 1759-1765.
30. He, H.W., R. Xiong, and J.K. Peng, *Real-time estimation of battery state-of-charge with unscented Kalman filter and RTOS mu COS-II platform.* Applied Energy, 2016. **162**: p. 1410-1418.
31. Li, X.Y., et al., *A simplified multi-particle model for lithium ion batteries via a predictor-corrector strategy and quasi-linearization.* Energy, 2016. **116**: p. 154-169.

32. Chen, Y., et al., *A graph-theoretic framework for analyzing the speeds and efficiencies of battery pack equalization circuits.* International Journal of Electrical Power & Energy Systems, 2018. **98**: p. 85-99.
33. Dang, X.J., et al., *Open-circuit voltage-based state of charge estimation of lithium-ion power battery by combining controlled auto-regressive and moving average modeling with feedforward-feedback compensation method.* International Journal of Electrical Power & Energy Systems, 2017. **90**: p. 27-36.
34. Yang, J.F., et al., *Online state-of-health estimation for lithium-ion batteries using constant-voltage charging current analysis.* Applied Energy, 2018. **212**: p. 1589-1600.
35. Yang, D., et al., *A novel Gaussian process regression model for state-of-health estimation of lithium-ion battery using charging curve.* Journal of Power Sources, 2018. **384**: p. 387-395.
36. Xia, B.Z., et al., *State of charge estimation of lithium-ion batteries using optimized Levenberg-Marquardt wavelet neural network.* Energy, 2018. **153**: p. 694-705.
37. Tanaka, T., et al., *Accurate and versatile simulation of transient voltage profile of lithium-ion secondary battery employing internal equivalent electric circuit.* Applied Energy, 2015. **143**: p. 200-210.
38. Wei, Z.B., et al., *Comparative study of methods for integrated model identification and state of charge estimation of lithium-ion battery.* Journal of Power Sources, 2018. **402**: p. 189-197.
39. Wang, S.L., et al., *Online dynamic equalization adjustment of high-power lithium-ion battery packs based on the state of balance estimation.* Applied Energy, 2016. **166**: p. 44-58.
40. Zhou, D.M., et al., *Online Estimation of Lithium Polymer Batteries State-of-Charge Using Particle Filter-Based Data Fusion With Multimodels Approach.* Ieee Transactions on Industry Applications, 2016. **52**(3): p. 2582-2595.
41. Wijewardana, S., R. Vepa, and M.H. Shaheed, *Dynamic battery cell model and state of charge estimation.* Journal of Power Sources, 2016. **308**: p. 109-120.
42. Wei, Z.B., et al., *Online monitoring of state of charge and capacity loss for vanadium redox flow battery based on autoregressive exogenous modeling.* Journal of Power Sources, 2018. **402**: p. 252-262.
43. Wang, S.L., et al., *Open circuit voltage and state of charge relationship functional optimization for the working state monitoring of the aerial lithium-ion battery pack.* Journal of Cleaner Production, 2018. **198**: p. 1090-1104.
44. Zou, Y., et al., *State-space model with non-integer order derivatives for lithium-ion battery.* Applied Energy, 2016. **161**: p. 330-336.
45. Wang, S.L., et al., *A novel safety anticipation estimation method for the aerial lithium-ion battery pack based on the real-time detection and filtering.* Journal of Cleaner Production, 2018. **185**: p. 187-197.
46. Shen, Y.Q., *Improved chaos genetic algorithm based state of charge determination for lithium batteries in electric vehicles.* Energy, 2018. **152**: p. 576-585.
47. Rahbari, O., et al., *A novel state of charge and capacity estimation technique for electric vehicles connected to a smart grid based on inverse theory and a metaheuristic algorithm.* Energy, 2018. **155**: p. 1047-1058.
48. Wang, S.L., et al., *Adaptive State-of-Charge Estimation Method for an Aeronautical Lithium-ion Battery Pack Based on a Reduced Particle-unscented Kalman Filter.* Journal of Power Electronics, 2018. **18**(4): p. 1127-1139.
49. Meng, J.H., et al., *Low-complexity online estimation for LiFePO4 battery state of charge in electric vehicles.* Journal of Power Sources, 2018. **395**: p. 280-288.
50. El Mejdoubi, A., et al., *State-of-Charge and State-of-Health Lithium-Ion Batteries' Diagnosis According to Surface Temperature Variation.* Ieee Transactions on Industrial Electronics, 2016. **63**(4): p. 2391-2402.
51. Lai, X., Y.J. Zheng, and T. Sun, *A comparative study of different equivalent circuit models for estimating state-of-charge of lithium-ion batteries.* Electrochimica Acta, 2018. **259**: p. 566-577.

(1) A novel comprehensive state of charge estimation method for the lithium-ion battery pack.
(2) The state of balance and aging process correction is considered in the recommended method.
(3) The estimation model is conducted by using the improved unscented Kalman filter.
(4) The improved variation coefficient is introduced to evaluate the cell-to-cell consistency.